TASK-DEPENDENT SELECTION OF GRASP KINEMATICS AND STIFFNESS IN HUMAN OBJECT MANIPULATION

Jason Friedman and Tamar Flash

(Department of Computer Science and Applied Mathematics, Weizmann Institute of Science, Rehovot, Israel)

Abstract

Object manipulation with the hand is a complex task. The task has redundancies at many levels, allowing many possibilities for the selection of grasp points, the orientation and posture of the hand, the forces to be applied at each fingertip and the impedance properties of the hand. Despite this inherent complexity, humans perform object manipulation nearly effortlessly. This article presents experimental findings of how humans grasp and manipulate objects, and examines the compatibility of grasps selected for specific tasks. This is accomplished by looking at the velocity transmission and force transmission ellipsoids, which represent the transmission ratios of the corresponding quantity from the joints to the object, as well as the stiffness ellipsoid which represents the directional stiffness of the grasp. These ellipsoids allow visualization of the grasp Jacobian and grasp stiffness matrices. The results show that the orientation of the ellipsoids can be related to salient task requirements.

Key words: grasping, object manipulation, stiffness

Introduction

Tools are believed to be part of the cause and effect of the evolution of increased intelligence in humans (Washburn, 1960). Tools allowed our human ancestors to effectively hunt, perform manual work, gather and process food and express creative impulses, which in turn led to the evolution of more advanced society. Using tools, we can extend our bodies and adjust the force and power of our muscles (Vogel, 2001). There is evidence from single neuron recordings in the monkey's brain and behavioral performance in normal and brain-damaged humans that tools can be incorporated into a plastic neural representation of our body (Maravita and Iriki, 2004). The interface for most tools is the hand, which is capable of holding the tool, and using it appropriately to interact with objects in a wide variety of ways. To use the tool in a purposeful way for a particular object and task, the central nervous system (CNS) must select the grasp points at which the fingers hold the object, as well as the posture of the hand. In addition, the impedance properties, which determine the stability of the grasp, must also be appropriately selected and tuned in order to successfully perform the interaction task.

Grasp selection in humans is largely subconscious. Despite the lack of conscious attention we give it, grasp selection in the kinematically redundant system of the hand poses a difficult problem, in that the requirements of a grasp are not clearly specified and it is difficult to define how to generate a grasp in order to best fulfill a given set of properties. This epitomizes the degrees of freedom problem of Bernstein (1967),

due to the larger number of degrees of freedom available in the hand than are necessary for stably grasping an object. In the field of robotics, a large body of literature deals with this question of grasp synthesis [see Shimoga (1996) for a review], which is a testimony to the complexity of the problem.

The study of grasping movements in humans has been mostly addressed from the perspective of reach-to-grasp movements, which have been considered as consisting of two independent components (Jeannerod, 1981) although several experimental studies have shown that external perturbations affect both channels (Haggard, 1994; Soechting and Flanders, 1993). Other studies of grasping movements have mostly focused on grasping kinematics (Mason et al., 2001; Santello et al., 2002; Kamper et al., 2003) or on force distribution among different fingers during object manipulation demonstrating the existence of different force distribution and coordination schemes such as enslaving and force sharing (Zatsiorsky et al., 1998; Danion et al., 2003).

Earlier studies have shown that the kinematic properties of both arm transport and grasp selection are influenced by the object and task properties (Marteniuk et al., 1987; Jakobson and Goodale, 1991). Intrinsic object properties that cause a particular type of interaction are known as affordances (e.g., the size, shape or weight of an object) and it was found that all the affordances of an object and not only those directly implicated influence the grasp being selected (Gentilucci, 2002).

To classify the large number of grasps used by humans, grasp taxonomies have been defined. Such

taxonomies are mainly based on the shape (i.e., power *vs.* precision grips) rather than the function of the grasp (Cutkosky, 1989), with further subdivisions based on the number of fingers being used and the prehension aperture. Arbib et al. (1985) and Iberall (1997) presented a virtual finger schema, whereby several fingers act together and can be modeled as a single "virtual" finger. Further grasp characterizations included that of Elliot and Connolly (1984) which divided manipulative hand movements into simultaneous and sequential ones.

Grasp formation and manipulation by the fingers require coordination of many degrees of freedom. Motor primitives, which are a basic set of movements that might subserve as building blocks for more complex movements, may present a simplifying strategy for grasp planning. Several different approaches to the use of primitives in grasping have been considered in robotics, where primitives have been proposed that operate in joint space (Speeter, 1991) or in Cartesian task space (Riley and Atkeson, 2002). Concerning primitives for human grasping, it has been suggested that they may consist of stored postures (Rosenbaum et al., 1995, 2001; Meulenbroek et al., 2001). A movement between the start and end postures is then computed (Rosenbaum et al., 2001). Smeets and Brenner (1999, 2002) claimed that a much simpler model is sufficient for planning grasping movements. Their model was based on determining the final locations of the fingertips of the thumb and index finger on the object, and then planning the trajectory that takes the fingertips to those locations. In addition to describing the kinematics of the movement, primitives may also define the applied forces and the dynamic properties of the grasp. One other prominent approach in robotics for programming robotic hands to perform compliant tasks has been to specify the task frame in which the manipulation can be defined and the constraints on forces and motions in this frame (Mason, 1981; De Schutter and Van Brussel, 1988).

The aforementioned taxonomies suggested for human grasping may enable classification of the movements into different subclasses, although it is unclear whether it is possible to decompose these grasps further into more elementary building blocks. In the past few years, with the development of devices such as the CyberGlove (Immersion), the finer kinematic details of human grasping have been studied, in particular, the selection of finger tip locations and joint angles. Principle component analysis (PCA) and related techniques for dimensionality reduction have been employed for inferring the underlying joint angle synergies during grasping (Santello et al., 1998, 2002; Mason et al., 2001; Zacksenhouse and Marcovici, 2001).

In the robotics literature, grasp synthesis is usually achieved by optimizing some quality measure (Shimoga, 1996). Many of these measures are based on the grasp Jacobian, G_h, which defines the relationship between the finger joint velocities, and the velocity of the object being grasped. The grasp Jacobian can be visualized by means of the manipulability ellipsoid (Yoshikawa, 1985), which represents the transmission properties of both velocities and forces between the joints and the object. Object velocity can be optimally produced along the major axis of the velocity transmission ellipsoid, and most accurately controlled along the minor axis. The analogous force transmission ellipsoid can also be derived from the grasp Jacobian. Chiu (1988) defined a measure known as the task compatibility index, which measures the transmission ratio of force or velocity along the direction required by the task. This is calculated as the square of the length of a vector in this direction from the center of the ellipsoid to the surface of the relevant force or velocity transmission ellipsoid. For a given task, Li and Sastry (1988) defined an ideal task ellipsoid whose shape (i.e., the relative lengths of the axes) is determined based on the relative force requirements in the different directions.

Grasping involves more than the placement of the fingers on the object. Due to the redundancy of the hand, the same grasp points on an object can in general be realized in many ways, thus influencing the stability and manipulability of the grasp. Both the stability and the manipulability of a grasp are affected by the grasp impedance. Impedance describes the relationship between externally applied forces and motion. It consists of a static component, the stiffness, which relates forces to displacements, and dynamic components, the damping and inertia, which relate forces to velocity and acceleration, respectively. The passive and active impedances of the human hand help to deal with changes in grasping conditions (Kao et al., 1997). Control of the dynamic behavior during manipulation requires control of the impedance of the hand (Hogan, 1985).

Earlier studies of upper limb impedance have focused mainly on measurements and characterization of the arm stiffness field while maintaining different arm postures in the horizontal plane (Mussa-Ivaldi et al., 1985; Flash and Mussa-Ivaldi, 1990; Tsuji et al., 1995). While maintaining posture, a manipulandum was used to introduce small displacements of the subject's hand in different directions. The resultant measured restoring forces, together with the measured end-point displacements were used to calculate the hand stiffness matrix and ellipse (Mussa-Ivaldi et al., 1985) which is characterized by three parameters: its size, shape and orientation. Techniques have also been developed for measuring stiffness during both loaded and unloaded movements (Gomi and Kawato, 1996, 1997; Burdet et al., 2000).

Compared to studies of whole arm stiffness, relatively few studies have focused on finger and hand stiffness. Hajian and Howe (1997) measured the impedance properties (i.e., stiffness, viscosity

and inertia) of the outstretched index finger's metacarpophalangeal joint (MPJ). Milner and Franklin (1998) studied the effects of finger posture and the direction of the voluntary forces on the resultant finger stiffness ellipses. Unlike for the stiffness of a single joint, where a monotonic relationship was found between joint stiffness and joint torque (Hajian and Howe, 1997), no systematic relationship was found for the whole finger. These authors concluded therefore that finger stiffness can most easily and robustly be controlled by altering the finger posture. Kao et al. (1997) measured the stiffness of the thumb and index finger in a plane. The two-dimensional stiffness of a grasp composed of these two fingers was calculated, and measures from the robotics literature were used to predict the properties of the grasp under external loads. The stiffness of an external object being grasped was measured by Van Doren (1998) and Buttolo (1996). These were used to consider the stiffness properties of different finger placements (Buttolo, 1996) and the effect of finger span and grasp force (Van Doren, 1998).

When considering grasping in three dimensions, a stiffness ellipsoid rather than an ellipse is appropriate. The derivation of the grasp stiffness ellipsoid from the stiffness ellipses of the fingertips is described in the analysis section. Lin et al. (2000) defined a frame-invariant stiffness based quality measure which quantifies the stability of the grasp. However, this measure can not take into account task specific stiffness requirements. Kim et al. (2004) defined a set of performance indices. These measures are normalized by dividing them by the difference between the maximum and minimum possible values and thus they are also non-dimensional. Different weights can be given to the different indices depending on the task.

In addition to the selection of grasp points, hand posture and stiffness, the distribution of forces applied by the fingers is controlled during grasping. Several phenomena, including enslaving and force sharing, have been observed (Zatsiorsky et al., 1998; Danion et al., 2003). Danion et al. (2003) modeled these phenomena with the mode hypothesis, where a mode is defined as the forces produced by all the fingers resulting from voluntary force production in a single finger. Multiple finger force production can then be modeled by the superposition of modes, with a weight factor dependent on the number of fingers used.

The present study is aimed at identifying and characterizing the dynamic and kinematic properties of different human grasps from a task perspective-namely what is common to different grasps in terms of hand shape and kinematic configuration as well as the forces and impedances which are selected in order to achieve grasp stability. In a recent review of the neural bases of complex tool use in humans it is argued that "we create complex artifacts (axes, pencils, spoons) that reflect a deep understanding of the physics of our bodies, the surrounding objects and the unique demands of the external environments we live in" (Johnson-Frey, 2004). Nevertheless, relatively few studies have attempted to provide comprehensive and more quantitative descriptions of the grasping and tool use strategies that humans use that may indeed reflect this deep understanding of the physics of grasping and object manipulation. Furthermore, while there have been a number of studies on postural hand synergies for tool use (Santello et al., 1998, 2002; Mason et al., 2001), few studies have measured and assessed the invariant characteristics of whole hand stiffness during grasping.

This article therefore focuses on proposing a description of multi-fingered pad opposition grasps (i.e., grasps using only the fingertips), in terms of their kinematic and stiffness properties, which define their interaction capabilities. This novel approach is based on measuring kinematic and stiffness properties of the individual fingers and combining them in order to predict the mechanical, i.e., both kinematic and dynamic properties of the grasp. These properties are examined in terms of the velocity transmission, force transmission and stiffness ellipsoids, which provide a task-level visualization of the compatibility of particular grasps for different tasks.

The velocity transmission characteristics (from the finger joints to the object) are visualized by the velocity transmission ellipsoid. The optimum direction for effecting a velocity (when the magnitude of the joint velocities vector is fixed) is along the major axis of the ellipsoid. The same notion also applies to forces. Finally, a grasp is most stiff (i.e., most resistant to external perturbations) in the direction of the major axis of the stiffness ellipsoid. The compatibility index in a particular direction is equal to the square of the distance from the center of the ellipsoid to the surface along the direction vector. The mathematical derivation of such ellipsoids is presented in the analysis section.

The predicted velocity and force capabilities of the grasp, as visualized by the ellipsoids, are related to the observed manipulations performed on the object during different tasks. It should be noted that the ellipsoids being considered here refer to the velocity, force and stiffness properties of the grasping hand and not of the arm. A more concise representation of the velocity and force transmission and stiffness ellipsoids based on their sizes, shapes and orientations, similar to the representation used for the upper arm stiffness during posture, is used for interpretation of the results. Common variations in these parameters among the different subjects and tasks are sought and are interpreted in view of the mechanical and functional requirements of the different grasping/manipulation tasks. We believe that such descriptions are necessary in order to gain better

understanding at both the behavioral and neural representation levels of the control and coordination strategies humans use during grasping and tool use.

METHODS

Subjects

Five right-handed and two left-handed male subjects aged between 25 and 37 (mean 31) gave informed consent to participate in the experiments. Stiffness measurements were not performed for one of the subjects.

Apparatus

The CyberGlove (Immersion) was used to measure 22 joint angles of the hand during the grasping movements. Each joint angle is measured by a sensor located over or near the finger joints and the wrist. The sensors are designed such that the raw sensor output has a linear relationship to the joint angle. The exact relationship is subject-dependent, hence a calibration procedure was performed to find the necessary values. The joint angles were sampled at 90Hz throughout the recordings, and smoothed using cubic splines. The 3D locations of the joints (including the fingertips) were estimated using a model of the hand based on the model presented in Turner (2001). Data analysis was performed using Matlab (Mathworks).

Simultaneously, the position and orientation of the wrist were recorded at 120Hz using the Fastrak (Polhemus), which records the 3D position and orientation by sensing an alternating current (AC) electro-magnetic field. The Fastrak data were resampled to 90Hz so that the data coincided with those from the CyberGlove. The Fastrak and CyberGlove data were combined to give the joint locations relative to the laboratory fixed reference frame. The joint locations were then transformed into a reference frame with its center located at the center of mass of the object.

During stiffness measurements, the CyberGrasp (Immersion) exoskeleton was placed on the subject's hand over the CyberGlove. The CyberGrasp base was attached with straps to the back of the hand, finger loops were placed on the medial phalanges and force applicator rings were placed over the fingertips. The force applicator rings are connected via "tendons" to the actuator enclosure (located in a box sitting on the table), which generates the required forces, updated at 1000Hz. Before use, the CyberGrasp was calibrated for each subject in order to create a mapping between the finger joint angles and the extension of the "tendons", so that the grasp controller can keep the tendons taut when no forces are applied.

Nine different grasps involving 5 different objects were tested. These grasps, shown in Table

TABLE I
The five objects and nine grasps tested in the experiment

Object	Dimensions	Grasps
Plastic cup	4.3 cm diameter at base, 8.3 cm diameter at top, 10.9 cm height	(1) Lift from side (*) (2) Lift from top (*)
Narrow jar	8 cm height of jar, 1.4 cm height of lid, 3 cm diameter	Unscrew lid Lift lid
Wide jar	5.6 cm height of jar, 1.5 cm height of lid, 6 cm diameter	(3) Unscrew lid (*) (4) Lift lid (*)
Teaspoon	13.7 cm length	(5) Lift (*) (6) Stir (*)

Note. Those marked with (*) were subject to detailed analysis. The lift grasp of the puzzle piece is not shown.

I, consisted of lifting a plastic cup, from the side and from the top, stirring with and lifting a teaspoon, unscrewing and lifting the lid of a narrow jar, unscrewing and lifting the lid of a wide jar and lifting a puzzle piece.

All the grasps in this study were pad opposition grasps, that is, grasps that contact the object only at the fingertips and not at the palm. The subjects were instructed to only use their fingertips (and not their palms), and adherence to this instruction was visually confirmed.

The experimental setup is shown in Figure 1. The subject sat upright next to a table, with his or her arm resting on the table at approximately waist level. Each trial began with the subject's hand at a marked starting position. The objects were manually placed at the marked object position before each manipulation. The objects were
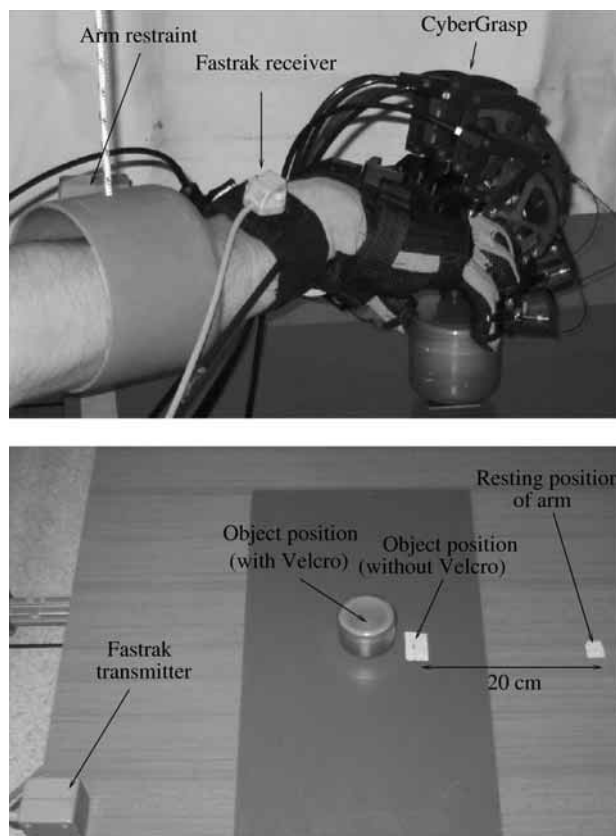
Fig. 1 – *Experimental setup. The appropriate object was placed at the marked position before each manipulation. When necessary, the object was attached to the table with strong Velcro (e.g., the base was attached to the table when unscrewing the lid). Joint angles of the hand were recorded by the CyberGlove worn on the hand, and the position and orientation of the wrist were measured with the Fastrak. During stiffness measurements, the CyberGrasp was placed over the CyberGlove and the forearm was restrained with a plastic loop.*

attached firmly to the table using strong Velcro during the stiffness measurement, and when the manipulation involved the lid of the object.

Procedure

The experiment was divided into two parts. The purpose of the first part was to measure the joint angles and wrist location and orientation at the onset of the manipulation task as well as during object manipulation. In the second part, the stiffness of the hand was estimated by asking the subjects to produce finger and hand configurations that matched those used at the onset of the manipulation task, and by applying forces to the fingertips and measuring their displacement.

The first part began with a procedure to calibrate the glove for the subject. Before each movement, the subject rested his or her arm on the table. Each trial, initiated by the experimenter when the subject was ready, began with a beep. The subject then moved his or her hand and held the object, and waited until the second beep (2.5 seconds later). He or she then manipulated the object for 2 seconds as instructed, after which a final beep was heard. At this time, he or she

returned the object to the table (if appropriate). For each object, the static arm, hand and finger configuration before the manipulation began (at the time of the second beep) were measured in order to calculate the grasp Jacobian. The manipulation with each type of grasp was repeated 3 times, i.e. 27 grasps were performed with the 9 manipulations. The first block of trials took approximately 20 minutes. Sufficient periods of rest were given to the subject between manipulations and at the end of the block.

After a short break, the second part began. The CyberGrasp (Immersion) was placed on the subject's hand over the CyberGlove, and the calibration procedure for the glove and CyberGrasp were performed. Each trial began with a beep, and in response the subject moved his or her hand in order to grasp the object and was instructed to maintain the initial posture they would use if they were to manipulate the object. Two seconds after the first beep, a second beep was generated. At this time, a force was applied to all fingers participating in the grasp for 300 msec, causing the fingers to move. After the 300 msec of force application, no force was applied, and the fingers returned to their initial position. At a random time, between 700 msec and 2000 msec after the end of the previous force application, another force was applied. A total of 25 forces were applied in each trial. During this entire procedure, the forearm was supported by a plastic loop hanging from a cantilever above. The displacements of the fingertips caused by the applied forces, generally between 5mm and 20mm, were calculated from the joint angles measured with the CyberGlove. The wrist sometimes moved slightly (up to 3mm) as a result of the force application.

Forces of 1.0N, 1.25N, 1.5N, 1.75N, 2.0N were applied. Each force was repeated 10 times with small variations added to the force (– .05N, – .025N, + 0N, + .025N, + .05N), each repeated twice. The small variations were used in order to prevent singular matrices in the calculations and derivations of the stiffness matrices. For each grasp, the forces were divided into two trials to prevent fatigue, i.e. 25 forces were applied within each trial.

Analysis

The position and orientation of the object during the manipulations in the first part of the experiment were not directly measured. Rather, they were calculated from the locations of the fingertips grasping the object relative to their location at the start of the movement, based on the assumption that the fingertips did not change position relative to the object. The position and orientation of the object were then described using Procrustes Analysis (implemented using the Statistics toolkit in Matlab), which finds the best

linear transformation of the fingers from the initial to the current position.

The grasp Jacobian at the start of the manipulation was calculated. Details of its derivation can be found in Murray et al. (1994) and in Shimoga (1996). The grasp Jacobian is the transformation from finger joint velocities to the velocity of the object. It takes into account the transformations for each finger from joint velocities to fingertip Cartesian velocity, the contact relationships (i.e., in which directions force can be transmitted from the fingertips to the object), and the transformations from the fingertip frames of reference to the object frame of reference. Thus it is a function of the hand posture and the lengths of the finger segments.

Velocity transmission ellipsoids and force transmission ellipsoids were constructed for the grasp at the start of each manipulation. These ellipsoids provide a visualization of the grasp Jacobian, The ellipsoids were generated separately for the translational and rotational velocities/forces.

The surface of the translational velocity transmission ellipsoid represents the object translational velocities that can be produced when the magnitude of the joint velocity vector (i.e., its Euclidean norm) is 1. The ellipsoid is defined by

$$\dot{x}_0^T \, (G_{h\,(trans)} \, G_{h\,(trans)}^T)^{-1} \, \dot{x}_0 \le 1$$

where $G_{h\,(trans)}$ is the translational part of the grasp Jacobian, and $\dot{x}_0$ is the object velocity. Similarly, the angular velocity ellipsoid is defined by

$$\omega_0^T \, (G_{h\,(angular)} \, G_{h\,(angular)}^T)^{-1} \, \omega_0 \le 1$$

where $G_{h\,(angular)}$ is the rotational part of the grasp Jacobian, and ω_0 is the object angular velocity.

The force transmission ellipsoids are defined by

$$F_0^T \, (G_{h\,(trans)} \, G_{h\,(trans)}^T) \, F_0 \le 1$$

where F_0 are the forces acting on the object. Similarly, the torque transmission ellipsoid is defined by

$$\tau_0^T \, (G_{h\,(angular)} \, G_{h\,(angular)}^T) \, \tau_0 \le 1$$

where τ_0 are the torques acting on the object. The direction with maximum velocity transmission ratio will also be the direction with minimum force transmission ratio. This relationship is a result of the conservation of energy – the work performed by the fingers results in the same amount of work performed on the object (excluding friction). These ellipsoids do not describe the actual velocity or force being applied, rather, they represent the velocity and force production capabilities of the grasp on the object as a function of the hand and finger configuration.

A first order model of stiffness was used in this research (i.e., damping and inertia terms were not considered), as was applied by Kao et al. (1997) and Milner and Franklin (1998) for measuring the finger's stiffness. Initially, the two dimensional stiffness matrix for each fingertip in the plane containing the major axes of the proximal, medial and distal phalanges was derived. The two dimensional Cartesian displacement of each finger was calculated based on the forward kinematics of the finger, in the coordinate system of the palm. The total displacement vector at the end of the 300 msec of force application was used. The direction of the applied force was assumed to be perpendicular to the major axis of the distal phalange and in the plane described above.

For each set of ten forces with approximately the same magnitude, the following equation was written:

$$\begin{bmatrix} F_{x_1} & \cdots & F_{x_{10}} \\ F_{y_1} & \cdots & F_{y_{10}} \end{bmatrix} = \begin{bmatrix} K_{11} & K_{12} \\ K_{21} & K_{22} \end{bmatrix} \begin{bmatrix} x_1 & \cdots & x_{10} \\ y_1 & \cdots & y_{10} \end{bmatrix}$$

i.e.,

$$F = Kx$$

Measurements where the fingers did not move, or moved in the opposite direction to the applied force were not used in calculating the stiffness. As a result of this, no stiffness matrices were generated for the tasks involving using the spoon for one of the subjects.

The parameters of the stiffness matrix K are found by solving the above equation in the least squares sense, under the condition that K is symmetric and positive definite. This was implemented using the Optimization toolbox of Matlab.

In order to determine the three dimensional stiffness matrix for each finger, the abduction stiffness was estimated. It was assumed that there is a linear relationship between applied force and stiffness, as observed in Hajian and Howe (1997). Based on Tables I and II from this paper, the extension and abduction stiffness were estimated to be

$$\begin{aligned} K_{ext} &= a_{ext}F_{ext} + c_{ext} \\ K_{abd} &= a_{abd}F_{abd} + c_{abd} \\ a_{ext} &= 40.9 \text{ m}^{-1} \\ c_{ext} &= 92.5 \text{ N/m} \\ a_{abd} &= 49.5 \text{ m}^{-1} \\ c_{abd} &= 126.0 \text{ N/m} \end{aligned}$$

where F_{ext} and F_{abd} are the applied extension and abduction forces, and K_{ext} and K_{abd} are the extension and abduction Cartesian stiffness.

Two stiffness ellipsoids were generated for each fingertip. The first uses the assumption that no force was applied in the abduction direction hence the abduction stiffness is 126.0 N/m. The second assumes that the maximal abduction force is applied. The maximum abduction force that can be applied without slipping can be calculated using the contact relationship, which is dependent on the coefficient of friction. It is assumed here that the coefficient of friction for all objects is $\mu = .45$,

TABLE II

Ellipsoid parameters for the mean (across subjects) velocity and force ellipsoids

	Azimuth (rad)	Elevation (rad)	Torsion (rad)	Volume	Shape 1	Shape 2
Cup lift (side)						
Transl. vel.	.15 (± .91)	.88 (± .15)	− 2.88 (± .94)	$3.60 (\pm 3.52) \times 10^6$	2.68 (± 1.21)	1.95 (± .72)
Ang. vel.	.16 (± 1.12)	.41 (± .30)	− 1.08 (± .34)	68.60 (± 47.88)	.61 (± .28)	1.17 (± 1.01)
Transl. force	− 1.30 (± .19)	− .13 (± .51)	1.56 (± .16)	$8.54 (\pm 2.07) \times 10^{-6}$	.72 (± .72)	1.35 (± .70)
Torque	1.45 (± .39)	− .71 (± .17)	− .39 (± .95)	.39 (± .20)	2.06 (± 1.56)	1.32 (± 1.31)
Cup lift (top)						
Transl. vel	− .92 (± .73)	.15 (± .39)	1.88 (± .15)	$3.37 (\pm .75) \times 10^6$	1.43 (± .53)	1.94 (± .89)
Ang. vel.	− .51 (± 1.02)	− .38 (± .19)	.22 (± 1.34)	43.89 (± 22.02)	2.28 (± 1.53)	2.53 (± .76)
Transl. force	− .14 (± .97)	− .90 (± .14)	1.90 (± .15)	$5.03 (\pm 1.99) \times 10^{-6}$	1.83 (± .46)	1.91 (± .90)
Torque	1.43 (± .33)	− .31 (± .11)	− 2.63 (± 1.55)	.56 (± .41)	2.56 (± 1.15)	3.59 (± 2.52)
Jar unscrew lid						
Transl. vel.	1.12 (± .82)	− .51 (± .27)	− .26 (± .81)	$5.36 (\pm 4.30) \times 10^6$	1.88 (± .54)	1.53 (± .19)
Ang. vel.	− 1.49 (± .29)	− .28 (± .19)	− 2.77 (± 1.51)	104.59 (± 134.49)	2.59 (± 1.23)	3.66 (± 1.56)
Transl. force	1.10 (± .76)	1.00 (± .18)	1.21 (± .47)	$5.22 (\pm 2.05) \times 10^{-6}$	1.17 (± .44)	1.34 (± .91)
Torque	.44 (± 1.03)	− .56 (± .10)	3.07 (± .87)	.39 (± .29)	1.49 (± .33)	4.69 (± 4.01)
Jar lift lid						
Transl. vel.	− 2.28 (± .62)	.44 (± .19)	.43 (± 1.12)	$2.36 (\pm 1.00) \times 10^6$	1.56 (± .44)	1.35 (± .57)
Ang. vel.	− .99 (± .64)	− .06 (± .17)	− .88 (± .55)	124.69 (± 131.51)	1.90 (± .91)	2.23 (± 1.10)
Transl. force	− .70 (± .86)	− .24 (± .38)	− 1.01 (± .33)	$8.56 (\pm 5.92) \times 10^{-6}$	.87 (± .41)	1.00 (± .63)
Torque	.67 (± .74)	− .90 (± .22)	2.29 (± .58)	.65 (± .91)	1.76 (± .79)	2.03 (± 1.21)
Spoon pickup						
Transl. vel.	.75 (± .91)	− 1.11 (± .08)	− 1.82 (± .73)	$2.77 (\pm .89) \times 10^6$	1.74 (± .38)	1.98 (± .73)
Ang. vel.	− 1.26 (± .40)	− .16 (± .31)	− 1.24 (± .61)	758.19 (± 778.05)	2.73 (± 1.60)	5.04 (± 3.39)
Transl. force	.61 (± 1.01)	.10 (± .29)	− 1.42 (± .38)	$7.33 (\pm 1.94) \times 10^{-6}$	1.42 (± .40)	2.05 (± .93)
Torque	.10 (± 1.20)	− 1.21 (± .05)	− 1.26 (± .64)	.04 (± .05)	3.72 (± 1.95)	4.22 (± 2.09)
Spoon stir						
Transl. vel.	1.11 (± 1.19)	1.08 (± .09)	1.43 (± .73)	$2.84 (\pm 2.43) \times 10^6$	1.52 (± .39)	2.21 (± .87)
Ang. vel.	− .65 (± 1.05)	.23 (± .38)	1.08 (± .17)	$1.15 (\pm .94) \times 10^3$	1.64 (± 1.14)	2.67 (± 2.77)
Transl. force	.59 (± .60)	− .12 (± .29)	− 1.65 (± .21)	$1.11 (\pm .75) \times 10^{-5}$	1.57 (± .30)	2.44 (± 1.09)
Torque	1.93 (± .70)	1.14 (± .04)	− .73 (± 1.54)	.28 (± .64)	3.71 (± 1.56)	2.56 (± .86)

Note. The orientations azimuth, elevation and torsion (in radians) define the direction in which force or velocity can be most efficiently affected, and the shape parameters (volume, shape1 and shape2) define the magnitude and degree of isotropy of velocity or force production. Volume is in $m^3 \, s^{-3}$, $rad^3 \, s^{-3}$, N^3 or $N^3 \, m^3$.

based on the reported skin-polythene coefficient of friction [from Figure 2a in Comaish and Bottoms (1971)]. This value was used as an approximation to the glove-object coefficient of friction, for which no data were available. The maximum abduction force that can be applied is then $F_{abd} = \mu F_{ext}$, under the assumption that the extension force is applied in the normal direction. Hence the maximal abduction stiffness using the above equations is

$$K_{abd} = \mu \, \frac{a_{abd}}{a_{ext}} (K_{ext} - c_{ext}) + c_{abd}$$

The assumption that the extension force is in the direction of the normal force is clearly violated in two cases: for the middle finger while stirring with the spoon, and for the last finger (ring or little finger, depending on the subject) while unscrewing the jar. In these cases, the normal force is in the abduction direction, and so the maximum abduction force will instead be $F_{abd} = \dfrac{F_{ext}}{\mu}$. Hence in these cases the maximum abduction stiffness was estimated as

$$K_{abd} = \frac{a_{abd}}{\mu \, a_{ext}} (K_{ext} - c_{ext}) + c_{ext}$$

The grasp stiffness matrix K_0 was then constructed from the finger stiffness matrices. A transformation is applied to each fingertip ellipsoid so that it will be in the same coordinate system as the object. Further details can be found in Cutkosky and Kao (1989) and in Murray et al. (1994). The grasp stiffness matrix is a 6×6 matrix. The upper left quadrant of this matrix represents the relationship between the translational forces and translational motion. This quadrant has been visualized as the translational stiffness ellipsoid. Similarly, the bottom right quadrant of the grasp stiffness matrix represents the relationship between angular motion and torques. This quadrant has been visualized as the rotational stiffness ellipsoid. The stiffness ellipsoids are visualized from the quadrant of the matrix by multiplying a hypothetical rotating input displacement (Mussa-Ivaldi et al., 1985):

$$k \begin{bmatrix} \cos(t_1)\sin(t_2) \\ \sin(t_1)\sin(t_2) \\ \cos(t_2) \end{bmatrix} 0 < t_1 < 2\pi, \; 0 < t_2 < \pi$$

The ellipsoids were described by six parameters. Three parameters represented the ellipsoids', orientations, consisting of a clockwise rotation of the major axis from the x axis about the z axis (elevation), followed by a clockwise rotation about the x axis (azimuth), followed by a clockwise rotation about the rotated major axis (torsion), all measured in radians. Due to the symmetry of an ellipsoid, the values were constrained to be between $-\pi/2$ and $\pi/2$. The three other parameters
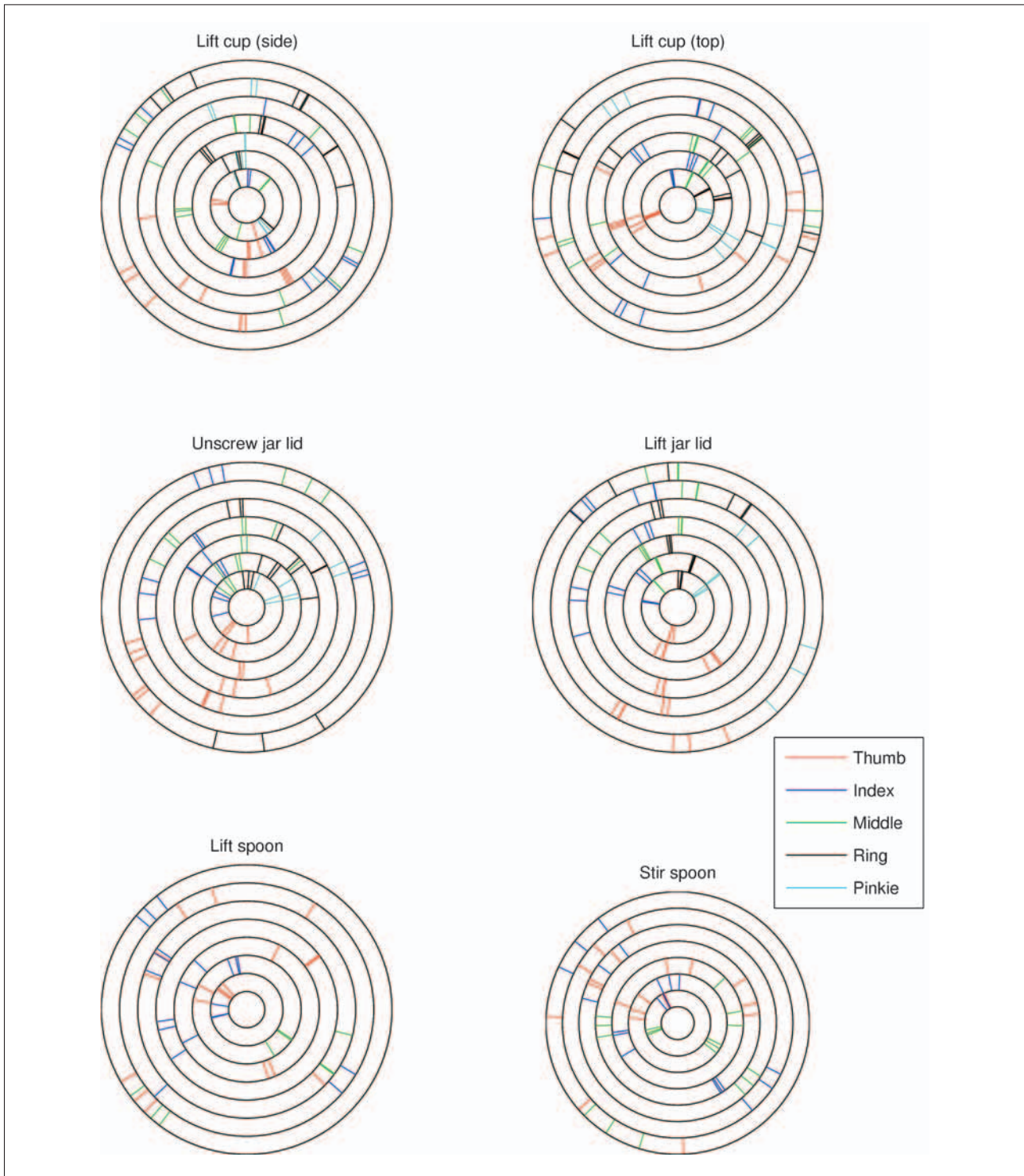
Fig. 2 – *Locations of the fingertips on the object for six tasks in the horizontal (XZ) plane. Each concentric circle represents a single subject. The position of a line represents the placement of the appropriate fingertip on the circumference of the object. Only fingers that participated in the grasp are plotted.*

represent the ellipsoids shapes and consisted of the volume of the ellipsoid, and the ratio of the major axis to the semi-major and minor axes, denoted by Shape 1 and Shape 2 respectively.

The task compatibility index defined by Chiu (1998) was computed for generating velocities and torques along the axes of the coordinate system. This is the square of the distance from the centre of the ellipsoid to the surface in the desired direction. For forces/torques, the task compatibility index C is defined by

$$C = 1/(u^T \, (G_h G_h^T) \, u)$$

and for velocities by

$$C = 1/(u^T \, (G_h G_h^T)^{-1} \, u)$$

where u is the desired force or velocity direction (in this case, along the coordinate axes).

The "mean" ellipsoids for each quantity and task of each subject were determined by taking the mean of the directions of the major axes, and the mean of the shape parameters. Ellipsoids with major axis directions that were more than two standard deviations away from the mean direction (in spherical coordinates), or shape parameters more than two standard deviations from the mean shape parameters were not used in computation of the mean ellipsoid. The same procedure was used for finding the mean ellipsoids across subjects.

<center>RESULTS</center>

Six of the grasps where patterns could be clearly observed are described in this section in detail (see Table I). For the sake of brevity, results were omitted for the narrow jar and puzzle piece. The fingertip positions on the objects for these grasps for all subjects are presented in Figure 2. The color of the line represents the finger used, and the location of the line on the circle represents the position of the fingertip on the surface of the object [projected onto the horizontal (XZ) plane]. As can be observed from this figure, for each type of manipulation, the subjects selected different postures, including when the same object was manipulated as part of different tasks. Differences were observed in the number of fingers used in the grasp (for example, when lifting the lid, the number of fingers used ranged between 3 and 5) and in the placement of the fingers (for example, significant variation was seen in the thumb position). Variation was often seen in the consecutive repetitions by the same subject, although this usually involved the same rotation of all the fingers relative to the object. The contact between the fingertips and the object was generally on the inner side of the finger, apart for unscrewing the lids and stirring the spoon, where the side of one finger was used.

The calculated fingertip stiffness matrices have diagonal elements ranging from approximately 50 N/m to 1000 N/m. These values are of a similar range to those observed in Kao et al. (1997) and Milner and Franklin (1998).

Qualitatively, observations on the grasp features were made based on the shape and orientation of the mean ellipsoids, represented by the parameters of the ellipsoids. The mean ellipsoids are presented graphically, in Figures 3 and 4, and their parameters are presented in Tables II and III. An approximate wire-frame rendering of the object is superimposed on the graphs of the ellipsoids to aid in the analysis. The orientation of the ellipsoid (defined by the azimuth, elevation and torsion parameters) determines the directions in which object velocity or force can be most efficiently actuated (for velocity and force ellipsoids respectively), or the direction of maximum stiffness

(for the stiffness ellipsoid). The shape parameters determine the isotropy of velocity or force production (for the velocity or force ellipsoids), or stiffness. If in some direction a large velocity can be generated on the object by the grasping fingers (with a unit joint velocity vector magnitude), in this direction the force that can be generated (with a unit joint torque vector magnitude) will be small. This is due to the principle of virtual work.

The distance from the center of the ellipsoid to the surface in a particular direction is a measure of how much velocity or force will be generated as a result of a unit joint velocity or torque vector (Chiu, 1988). The values of the compatibility index (which is the square of this distance) for all subjects for six grasps are plotted for force and velocity production (Figure 5) and for stiffness (Figure 6), along the x (left-right), y (vertical) and z (front-back) axes. The compatibility measures were calculated only along these axes because of their connection to axes of movement and force production involved in the manipulation tasks.

Significant differences in the compatibility index at the $p < .1$ and $p < .05$ levels between different tasks being performed on the same object are marked in the figures by (*) and (**) respectively. The comparison was performed using the Wilcoxon signed rank test (Gibbons, 1971) on the values of the compatibility index. When the compatibility index is consistently higher for one task compared to a second task being performed on the same object, this invariance may represent a task-related property of the grasp (for example, torque production about the vertical axis) that the CNS is trying to optimize.

<center>*Cup*</center>

A plastic cup, shaped like a truncated elliptical cone, was picked up with two different grasps, from the side (Task 1) and from the top (Task 2). In both cases, only the fingertips contacted the object, and not the palm. The movements involved lifting the cup vertically (along the positive y direction), generally with negligible rotation.

Lifting a cup primarily requires movement of the arm rather than the fingers. Hence, the role of the grasp is to stabilize the object and prevent undesirable movement. Lifting from the side generally involved placing the thumb on one side, and the other fingers close together (see Figure 2, top left). When lifting from the top, the subjects spread their fingers around the rim of the cup, although not uniformly. The values of the task compatibility indices in Figure 5 indicate that the two postures have different interaction capabilities with the object.

Lifting from the side has translational velocity compatibility indices in the x (left-right) and z (front-back) directions significantly smaller than those for lifting from the top (Figure 5, top row). A
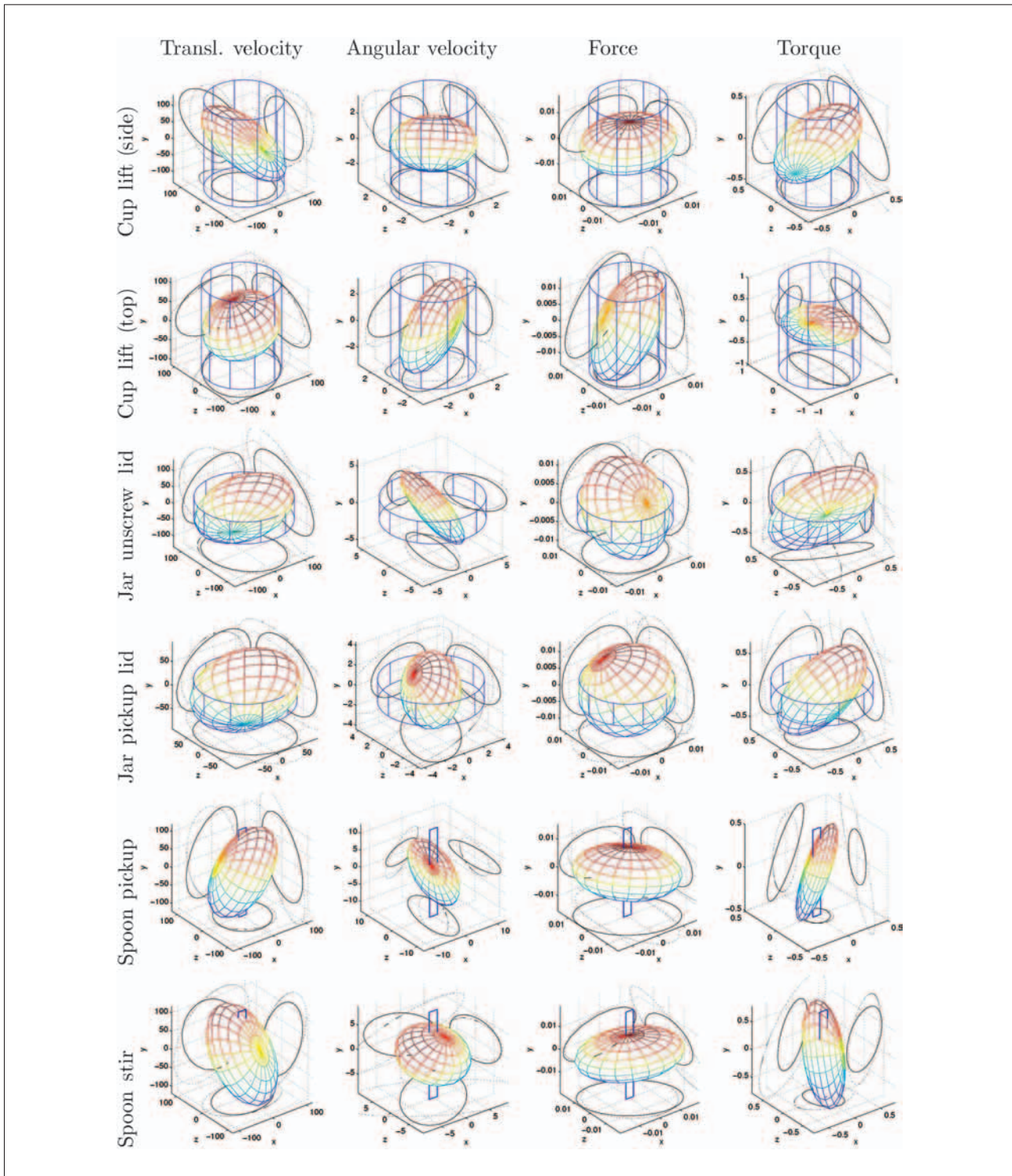
Fig. 3 – *Mean translational velocity (first column), angular velocity (second column), translational force (third column) and torque (fourth column) ellipsoids for lifting the cup from the side (first row) and from the top (second row), unscrewing (third row) and lifting (fourth row) the lid of a jar, and lifting (fifth row) and stirring with (sixth row) a spoon. The ellipsoids are the mean ellipsoids over the seven subjects. The solid and dashed black lines are the projections of the mean and the mean plus one standard deviation respectively onto the XY, YZ and XZ planes. A wire-frame not-to-scale rendering of the object is superimposed on the graphs. The distance from the centre of the ellipsoid to the surface in a certain direction is the amount of velocity (force) that can be produced as a result of a joint velocity (torque) vector with unit magnitude.*

significantly larger compatibility index is also observed in the x direction for the force variable for lifting from the side rather than from the top (Figure 5, third row). These results mean that when lifting from the side, larger forces can be produced in this direction.

Seemingly contradictory results are observed when considering the stiffness, where lifting from the top has a significantly higher translational stiffness compatibility index than lifting from the side in the z direction and generally higher translational stiffness although not statistically
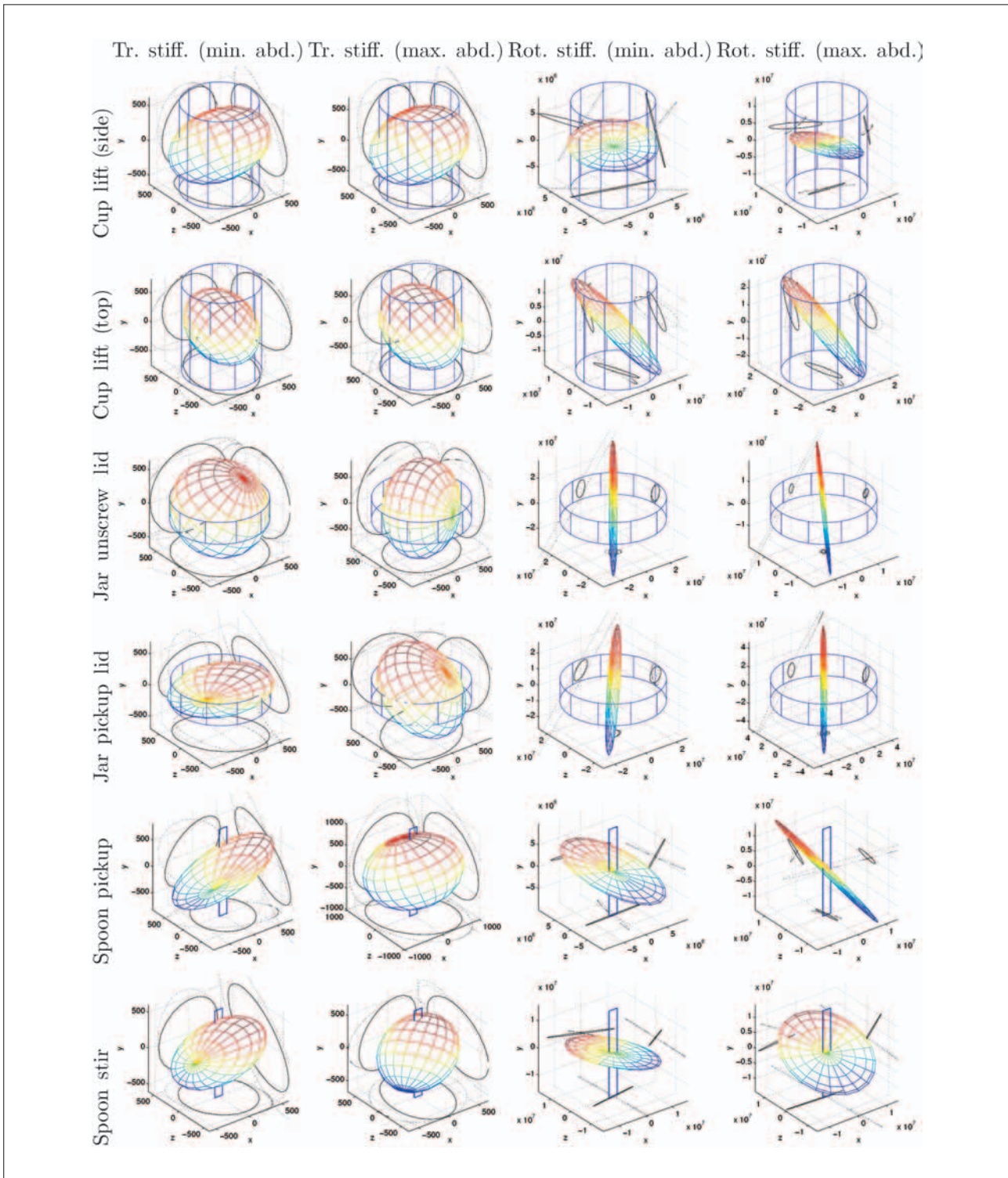
Fig. 4 – *Mean translational stiffness under the assumption of minimum (first column) and maximum (second column) abduction stiffness, and mean rotational stiffness for minimum (third column) and maximum (fourth column) abduction stiffness. The rows represent the same objects as in Figure 3. The stiffness ellipsoids represent the relative stiffness of the grasp in different directions.*

significant in the *x* direction. The explanation for this can be found in the fact that the grasp stiffness measures the response of the grasp to applied forces as a result of the elastic properties of the muscles, tendons and joints, rather than the ability of the grasp to actively generate forces.

In terms of angular velocities, lifting from the top has a significantly smaller task compatibility

index for angular velocity in the *y* and *z* directions than for lifting from the side, meaning that the velocity can be better controlled in these directions. Additionally, the rotational stiffness compatibility index in the *y* direction for both types of estimation of the abduction stiffness are considerably higher for lifting from the top. Thus, lifting from the top is able to better actively control angular velocities

TABLE III
Ellipsoid parameters for the stiffness ellipsoids

	Azimuth (rad)	Elevation (rad)	Torsion (rad)	Volume	Shape 1	Shape 2
Cup lift (side)						
Tr. stiff. (min. abd.)	1.08 (± 1.08)	− .60 (± .35)	1.78 (± .55)	$5.65 (\pm 1.60) \times 10^8$	1.97 (± .83)	1.70 (± .46)
Tr. stiff. (max. abd.)	1.13 (± 1.15)	− .63 (± .35)	1.62 (± .47)	$8.50 (\pm 3.17) \times 10^8$	1.97 (± .82)	1.59 (± .67)
Rot. stiff. (min. abd.)	− .06 (± .99)	.65 (± .23)	− .49 (± 1.03)	$4.39 (\pm 4.35) \times 10^{19}$	1.68 (± .95)	49.93 (± 50.20)
Rot. stiff. (max. abd.)	− .14 (± .74)	.57 (± .28)	2.72 (± 1.16)	$6.52 (\pm 6.77) \times 10^{19}$	4.69 (± 7.08)	49.53 (± 45.39)
Cup lift (top)						
Tr. stiff. (min. abd.)	− 1.26 (± .57)	.17 (± .41)	.61 (± 1.24)	$9.73 (\pm 9.40) \times 10^8$	1.30 (± .62)	1.52 (± .42)
Tr. stiff. (max. abd.)	− 1.26 (± .52)	.11 (± .31)	.61 (± 1.17)	$1.82 (\pm 2.01) \times 10^9$	1.14 (± .49)	1.35 (± .72)
Rot. stiff. (min. abd.)	.92 (± .83)	.83 (± .21)	1.15 (± .72)	$4.69 (\pm 6.10) \times 10^{20}$	22.03 (± 27.75)	3.05 (± 4.14)
Rot. stiff. (max. abd.)	1.05 (± .80)	.88 (± .28)	1.17 (± .69)	$2.93 (\pm 5.54) \times 10^{21}$	14.53 (± 29.18)	3.39 (± 4.74)
Jar unscrew lid						
Tr. stiff. (min. abd.)	− .25 (± .91)	.18 (± .35)	1.03 (± .37)	$1.09 (\pm 1.05) \times 10^9$	.96 (± .56)	1.03 (± .86)
Tr. stiff. (max. abd.)	− .30 (± 1.09)	.34 (± .32)	.11 (± .88)	$1.63 (\pm 1.10) \times 10^9$	.83 (± .29)	1.12 (± .91)
Rot. stiff. (min. abd.)	− .92 (± .98)	− .80 (± .14)	− 1.49 (± .69)	$2.55 (\pm 5.56) \times 10^{21}$	17.88 (± 28.12)	10.28 (± 18.08)
Rot. stiff. (max. abd.)	− 1.05 (± 1.07)	− .82 (± .17)	− 1.53 (± .64)	$1.26 (\pm 1.09) \times 10^{20}$	32.93 (± 52.68)	19.85 (± 23.08)
Jar lift lid						
Tr. stiff. (min. abd.)	1.01 (± .51)	− .33 (± .38)	− 2.94 (± .95)	$6.43 (\pm 3.97) \times 10^8$	2.14 (± 1.49)	1.56 (± .55)
Tr. stiff. (max. abd.)	− .37 (± 1.15)	.33 (± .28)	.78 (± .79)	$1.97 (\pm 2.35) \times 10^9$	1.02 (± .16)	1.54 (± .77)
Rot. stiff. (min. abd.)	− .82 (± .86)	− .85 (± .11)	− 1.11 (± .72)	$1.58 (\pm 3.35) \times 10^{21}$	11.47 (± 14.80)	11.24 (± 20.56)
Rot. stiff. (max. abd.)	− .92 (± .82)	− .88 (± .11)	− 1.36 (± .66)	$3.59 (\pm 7.71) \times 10^{21}$	21.99 (± 29.30)	12.20 (± 22.02)
Spoon pickup						
Tr. stiff. (min. abd.)	1.06 (± .10)	− .72 (± .08)	3.00 (± .85)	$1.02 (\pm 1.16) \times 10^9$	2.83 (± 2.23)	2.13 (± .12)
Tr. stiff. (max. abd.)	1.00 (± .24)	− .41 (± .21)	− 1.56 (± .09)	$2.88 (\pm 4.70) \times 10^9$	1.54 (± .68)	1.50 (± .52)
Rot. stiff. (min. abd.)	.38 (± .78)	.63 (± .26)	− 2.50 (± 1.41)	$3.98 (\pm 5.43) \times 10^{19}$	2.59 (± 4.06)	78.93 (± 70.94)
Rot. stiff. (max. abd.)	.95 (± .61)	.76 (± .20)	2.44 (± 1.40)	$1.13 (\pm 1.93) \times 10^{20}$	5.93 (± 10.63)	56.40 (± 42.25)
Spoon stir						
Tr. stiff. (min. abd.)	1.26 (± .07)	− .71 (± .05)	− 3.01 (± .85)	$5.33 (\pm 4.99) \times 10^8$	2.04 (± .87)	1.75 (± .35)
Tr. stiff. (max. abd.)	1.47 (± .02)	− .38 (± .11)	− .79 (± .70)	$6.27 (\pm 4.65) \times 10^8$	1.75 (± .58)	1.26 (± .19)
Rot. stiff. (min. abd.)	.18 (± 1.11)	.43 (± .31)	.69 (± 1.34)	$5.38 (\pm 6.07) \times 10^{19}$	3.64 (± 2.99)	122.79 (± 85.09)
Rot. stiff. (max. abd.)	.44 (± .69)	.55 (± .34)	− 2.49 (± 1.42)	$1.30 (\pm 1.96) \times 10^{20}$	1.41 (± .98)	94.85 (± 65.35)

Note. Interpretation of the parameters is the same as Table II. Units of volume are N^3 and $N^3 m^3$.

about the y axis and additionally passively respond to external disturbances about this axis. It appears that the choice of grasping from the side or top should depend on whether translational or rotational disturbances are more likely.

The rotational stiffness ellipsoids were highly anisotropic, long and thin, with low stiffness in the z direction for lifting from the side and in the x direction for lifting from the top (see Figure 4, first two rows, third and fourth columns). The direction of the major axis was roughly perpendicular to the direction of the opposition axis, defined here as the line connecting the thumb and the average of the other fingers positions. The rotational stiffness ellipsoids were similar for both cases of abduction stiffness.

Wide Jar

Two grasps were performed on the wide jar - unscrewing the lid (task number 3), and lifting the lid after it was already unscrewed (task number 4). It was observed that unscrewing the lid involves primarily an anti-clockwise rotation about the y axis. Lifting the lid, in contrast, involves a translation in the positive y direction, with negligible rotation.

For lifting the lid, the subjects generally placed their thumbs on the side of the object closest to their chest (in the lower part of the circle, in Figure 2), and the other fingers on the other side of the object,

relatively close to each other with even spacing between the fingers. When unscrewing the same lid, the thumb was rotated clockwise, and the last finger used in the grasp was placed such that the contact with the object was with the side of the finger.

In order to unscrew the lid, it is necessary to apply a torque about the y axis. Although the difference in the orientation of the torque ellipsoids for unscrewing and lifting the lids is small, the task compatibility index for applying a torque in the y axis is significantly larger for the unscrewing task than for the lifting task ($p < .05$).

The difference in torque production capabilities of the two grasps is due to the different finger placement. The placement of the last finger used in the grasp such that it contacts the object with the side of the finger allows rotation of the object by this finger by the extension of three joints (metacarpophalangeal, proximal and distal interphalangeal) rather than only by the abduction of the MPJ. In addition, the rotation of the thumb clockwise on the object moves it closer to its limit such that it can rotate the lid over a larger angle.

The clear difference in task compatibility observed for torque production in the y direction is not observed for translational velocity or force production in this direction. Varied results were observed regarding the grasp for which translational velocity in the vertical (y) direction can be more efficiently produced.
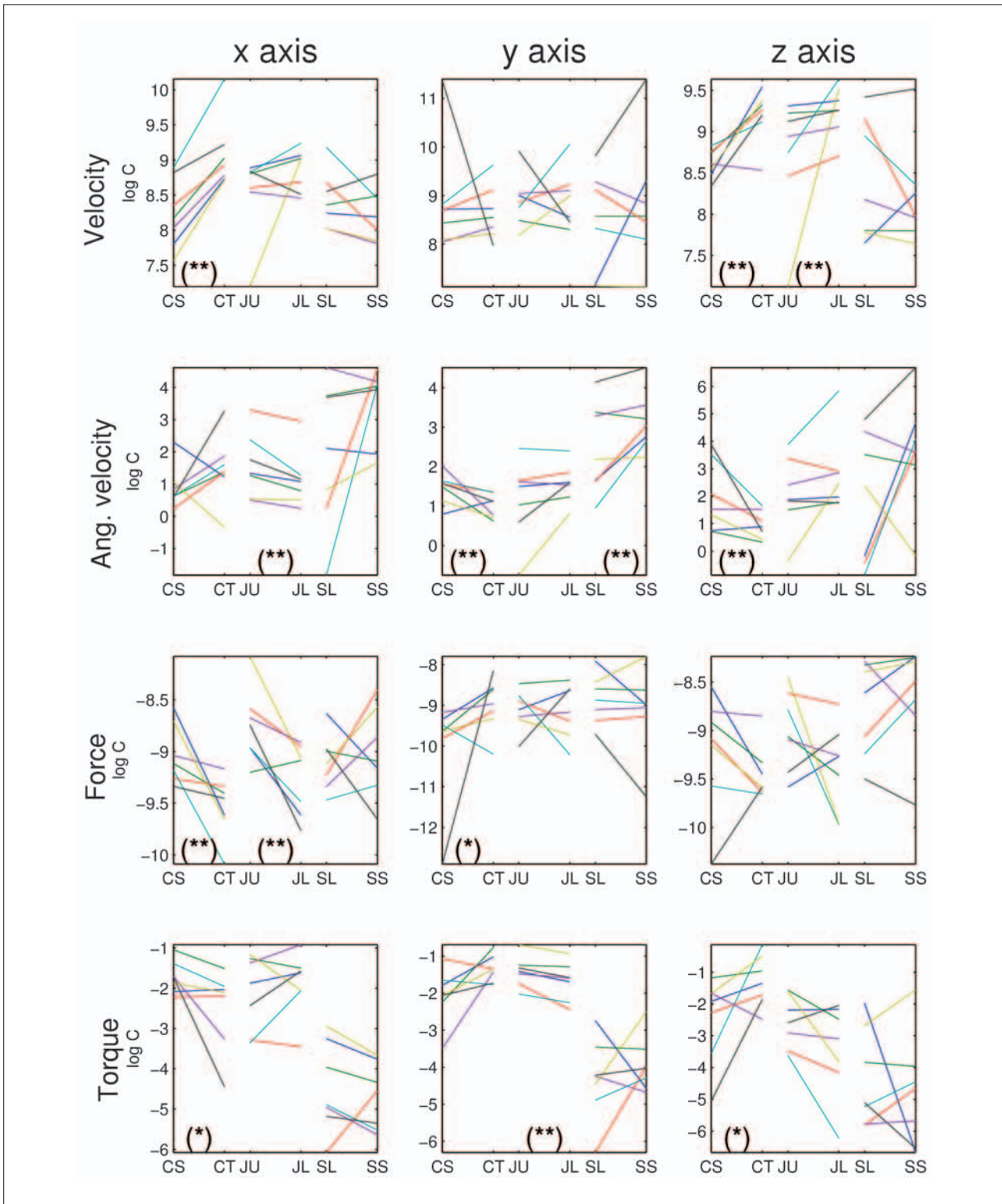
Fig. 5 – *Kinematic task compatibility indices. The task compatibility indices for translational velocity (first row), angular velocity (second row), translational force (third row) and torque (fourth row) along the x (first column), y (second column) and z (third column) directions, for lifting the cup from the side (CS) and top (CT), unscrewing (JU) and lifting (JL) the lid of the jar, and lifting (SL) and stirring (SS) with the spoon. Log scales are used on the graphs. Lines join different actions on the same object. (*) and (**) represent significantly different values at p < .1 and p < .05 levels on the Wilcoxon signed rank test between the two actions performed on the object.*

The translational stiffness ellipsoids observed differ between the two tasks. While for unscrewing the lid (task number 3) the stiffness ellipsoids are fairly isotropic, i.e., the values of shape1 and shape2 are close to 1, the stiffness ellipsoids are "flatter" for lifting the lid, with greater stiffness in the horizontal (*x* and *z*) directions. These stiffness values are large in a direction perpendicular to the velocity involved in lifting, which is along the vertical (*y*) direction. The translational stiffness
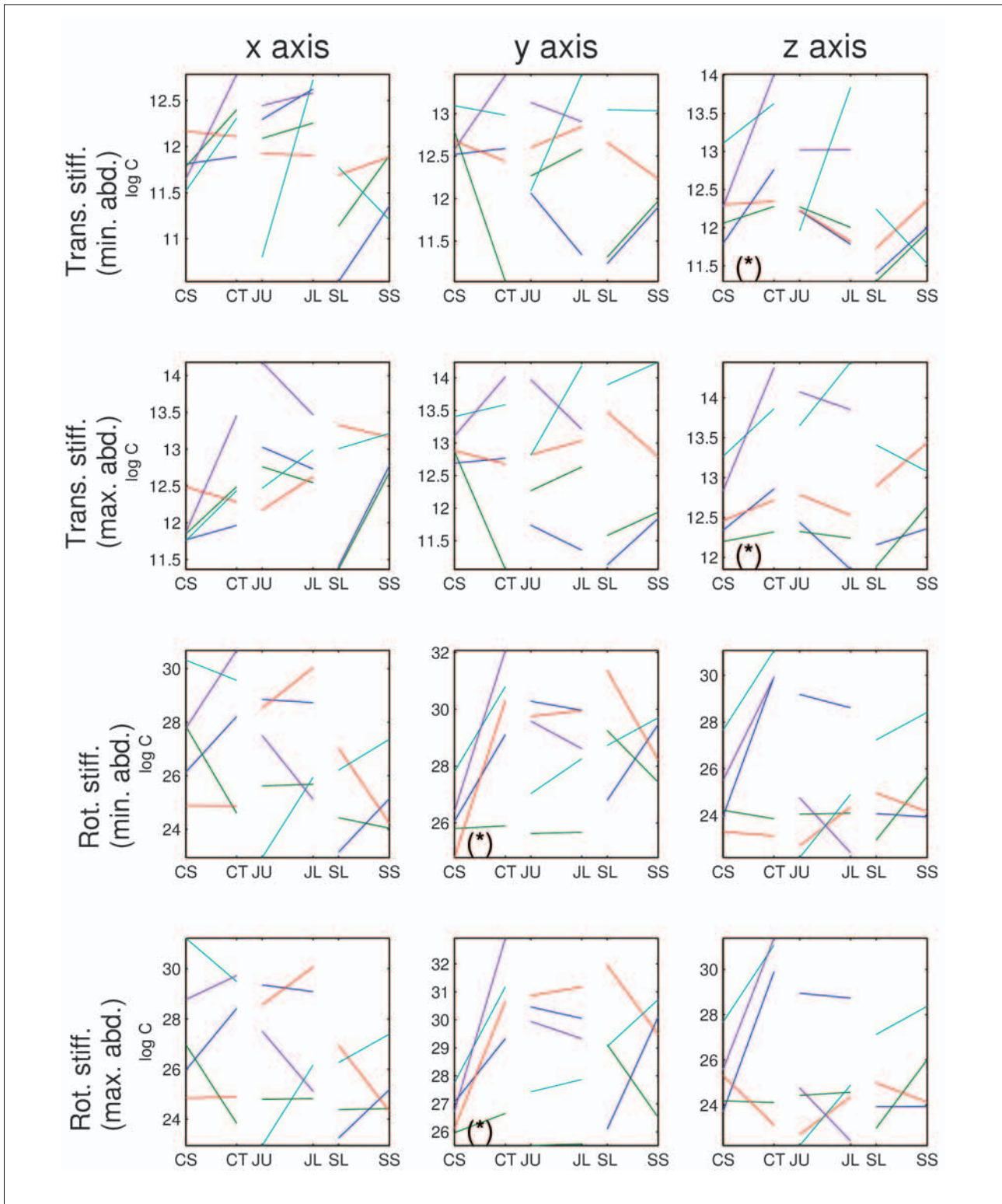
Fig. 6 – *Stiffness task compatibility indices. The format of the graphs is the same as in Figure 5.*

ellipsoids with minimum and maximum abduction stiffness have similar shape and orientation, although the volume of the ellipsoids with maximum abduction stiffness is significantly larger.

The mean rotational stiffness ellipsoid has greater stiffness in the vertical (*y*) direction for both types of grasp, which would appear to be counterproductive for torque production about this

axis. However, large amounts of variation were observed in the rotational stiffness for this task.

Spoon

Two different types of manipulation were performed with the spoon: lifting the spoon (task number 5), and stirring with the spoon (task

number 6). Whereas the task of lifting the spoon vertically (in the *y* direction) is primarily performed by the arm, stirring the spoon [generally about the vertical (*y*) axis] was performed by movements of the fingers.

For lifting the spoon, subjects used two or three fingers. Large amounts of variation were observed in the placement of the fingers on the spoon. All subjects apart from one (who used two fingers) used three fingers for stirring with the spoon. Generally, the spoon was grasped with the side of the middle finger. Stirring with the spoon was significantly better for applying an angular velocity, about the vertical (*y*) axis than for lifting the spoon. It should be noted that this is different from the unscrewing of the lid where a preference was observed for applying torque about the *y* axis. In contrast, the best grip for applying an angular velocity along the *x* and *z* axes varied greatly between subjects.

Stiffness ellipsoids were not constructed for one subject due to insufficient movement of the fingers resulting from the force application. The translational stiffness ellipsoids for stirring and lifting the spoon were fairly isotropic, although the volume of the translational stiffness ellipsoid for lifting the spoon was much larger than that for stirring with the spoon although two fingers were generally used for picking up the spoon as opposed to three for stirring with it. This finding reflects the different task requirements of the grasps, because for lifting the spoon the grasp is required only to hold securely the object while lifting is performed by the arm.

DISCUSSION

The use of a tool or manipulation of an object requires that certain movements and forces be applied to the object or tool. The redundancy of the kinematic degrees of freedom within the hand means that in general many grasps can be selected that satisfy the basic need for grasp stability. The grasp can be selected such that applying the desired motion or force can be performed in an efficient and accurate manner. In addition, the impedance properties of the grasp will affect the stability of the grasp, and how it handles errors. This work has attempted to describe how the selected grasp posture and stiffness affect the ability to manipulate objects and the suitability of the grasp for different manipulation tasks.

Throughout this work, the grasps have been analyzed in the frame of reference of the object. Various works in robotics [for example, Mason (1981) and De Schutter and Van Brussel (1988)] have proposed planning control of a robotic manipulator by specifying the task constraints in terms of the task frame. However, it is difficult to know what constraints need to be specified for a given task. For example, it is not intuitively clear whether it is more desirable to be able to generate a high angular velocity or torque in order to unscrew a lid. In this work, the goal is the inverse of that in robotics studies – to determine which characteristics humans give to grasps in order to perform different tasks.

The use of the velocity and force ellipsoids to measure task compatibility for generating optimum grasps for robotic manipulators was proposed by Chiu (1988). Buttolo (1996) compared the stiffness of different pen grasps by comparing the stiffness ellipsoids of the grasp. He found that different three fingered grasps gave similar stiffness ellipsoids, which were more suitable for fine control than using a single finger because of larger stiffness values.

For all of the tasks, a large amount of variation in finger placement on the objects was observed. The velocity and force transmission ellipsoids are a function of the hand posture, and so the variation in finger placement caused significant variations in the resulting velocity and force transmission ellipsoids. The grasp stiffness, as visualized by the stiffness ellipsoids is also dependent on the hand posture (as well as the finger stiffnesses). Thus, some of the variation in the stiffness ellipsoids was probably due to variations in the posture. However, despite these significant variations, patterns were observed in the compatibility of the grasps for controlling or effecting force and velocity in salient task directions. For example, a larger torque can be produced about the vertical (*y*) axis for unscrewing the lid of the jar rather than for lifting the lid. Based on this and similar findings, it appears that for the same object, different preferred directions of velocity and force production were selected depending on the task being performed. This is important to note, because it implies that grasp planning cannot be performed based purely on the geometry of the object but rather must take into account the desired manipulation.

Greater variance was observed in the task compatibility measures between subjects for some of the parameters where there was no obvious connection between the parameter and the task. This suggests that control or actuation of force or velocity in these directions is less important for a successful completion of the task.

For the rotational stiffness, the major axis of the stiffness ellipsoid was often perpendicular to the opposition axis (the line connecting the thumb and the average of the other finger positions). This may be a result of forces being applied parallel to this axis to hold the object stably.

The translational stiffness ellipsoids under the assumption of maximum abduction stiffness have a larger volume than the stiffness ellipsoids under the assumption of minimum abduction stiffness for the same task. This is because the finger stiffness ellipsoids under the assumption of maximum

abduction will have a larger volume, and the grasp stiffness ellipsoids are the result of the summation of the finger stiffness ellipsoids (after rotation into the appropriate frame of reference).

It appears that the stiffness may be selected by making the grasp compliant (i.e., low stiffness) in the directions in which forces or movement are to be applied, and stiff in the directions in which movement is not desired (Cutkosky, 1985). Using more fingers in a grasp will generally increase the stiffness. Although the net force on the object will be zero when the object is not moving (so that the object is in equilibrium), in spite of the "canceling out" of the applied forces, the stiffness of the fingers sum.

In the construction of the grasp stiffness ellipsoid, it was assumed that the fingers are not coupled. However, some of the muscles serve all fingers (Li et al., 2002; Leijnse, 1997). Hence, it is expected that there will be some coupling between the fingers. The magnitude of the coupling should be determined through further experiments.

Evidence for task-based grasp planning has been provided by neural recording studies. Neurons in behaving monkeys in area F5 (in the rostral part of inferior area 6) have been observed to show selectivity for different types of grasping, namely precision grip, finger prehension and whole-hand prehension (Rizzolatti et al., 1988). Area F5 is believed to be the monkey homologue of Broca's area in humans (Rizzolatti and Arbib, 1998). In area F2, in the caudal part of area 6, neurons were also observed that were selective for the type of grasp (Raos et al., 2004). These authors have suggested that these areas (F2 and F5) collaborate in the control of grasping. Jeannerod et al. (1995) suggested an explanation of the physiological data based on the idea of schemas. A schema was defined by these authors as populations of neurons in F5 that code for different types of manipulation or the selection of which fingers to use. Grasping and manipulation can be performed by the coordination of these schemas.

While the present work has described some of the features of several types of manipulation, much further work needs to be done to fully understand how humans select grasps in order to manipulate objects. First, the number of fingers selected for manipulation requires further investigation. Theoretical work in robotics has characterized the minimum number of fingers necessary for properties such as force closure [for example, Mishra et al. (1987)]. It is not clear how these results are reflected in the number of fingers selected by humans.

A source of uncertainty in the grasp model was introduced by the lack of measurements of the abduction stiffness. Measurements of the applied fingertip abduction forces would allow better modeling of the three dimensional fingertip stiffness and hence grasp stiffness. This may be possible using instrumented objects. Use of a full impedance model (including damping and inertia) could also contribute to the accuracy of the model.

The translational and rotational stiffness ellipsoids plotted provided visualizations of the upper left and lower right quadrants, respectively, of the grasp stiffness matrix. The upper right quadrant of the grasp stiffness matrix represents the relationship between angular motion and translational forces, while the lower left quadrant represents the relationship between translational motion and torques. Further analysis needs to be performed to examine the patterns observed in these quadrants and their relationship to the selected tasks being performed.

Features of a grasp, in addition to the velocity and force transmission and stiffness characteristics, such as the available joint movements and distances from singularities can be defined (Shimoga, 1996). Additional invariant properties of the grasps which are selected may be revealed by further investigation of such features. The grasp selection problem can also be considered as an optimization problem, where certain grasp quality measures are optimized. It would be of interest to compare hand postures and stiffness properties that optimize various grasp quality measures with observed postures and stiffness properties selected for manipulation.

The role of primitives in grasp selection is also unclear. While kinematic synergies have been observed in generating hand postures during grasping (Santello et al., 1998, 2002; Mason et al., 2001), such primitives need to be also related to the manipulation and dynamic properties of the grasp. This is also an important area for future investigation.

REFERENCES

ARBIB M, IBERALL T and LYONS D. Schemas that integrate vision and touch for hand control. In Arbib M and Hansen A (Eds), *Vision, Brain and Cooperative Communication*. Cambridge, MA: MIT Press, 1985.

BERNSTEIN N. *The Co-ordination and Regulation of Movements*. London: Pergamon Press, 1967.

BURDET E, OSU R, FRANKLIN D, YOSHIOKA T, MILNER T and KAWATO M. A method for measuring endpoint stiffness during multi-joint arm movements. *Journal of Biomechanics, 33:* 1705-1709, 2000.

BUTTOLO P. *Characterization of Human Pen Grasp with Haptic Displays*. Unpublished doctoral dissertation, University of Washington, 1996.

CHIU S. Task compatibility of manipulator postures. *International Journal of Robotics Research, 7:* 13-21, 1998.

COMAISH S and BOTTOMS E. The skin and friction: Deviations from Amonton's laws, and the effects of hydration and lubrication. *British Journal of Dermatology, 84:* 37-43, 1971.

CUTKOSKY M. *Robotic Grasping and Fine Manipulation*. Boston: Kluwer, 1985.

CUTKOSKY M. On grasp choice, grasp models, and the design of hands for manufacturing tasks. *IEEE Transactions on Robotics and Automation, 5:* 269-279, 1989.

CUTKOSKY M and KAO I. Computing and controlling the compliance of a robotic hand. *IEEE Transactions on Robotics and Automation, 5:* 151-165, 1989.

DANION F, SCHÖNER G, LATASH M, LI S, SCHOLZ J and ZATSIORSKY V. A mode hypothesis for finger interaction during multi-finger force-production tasks. *Biological Cybernetics, 88:* 91-98, 2003.

DE SCHUTTER J and VAN BRUSSEL H. Compliant robot motion I. A formalism for specifying compliant motion tasks. *International Journal of Robotics Research, 7:* 3-17, 1988.

ELLIOT J and CONNOLLY K. A classification of manipulative hand movements. *Developmental Medicine and Child Neurology, 26:* 283-296, 1984.

FLASH T and MUSSA-IVALDI F. Human arm stiffness characteristics during the maintenance of posture. *Experimental Brain Research, 82:* 315-326, 1990.

GENTILUCCI M. Object motor representation and reaching-grasping control. *Neuropsychologia, 40:* 1139-1153, 2002.

GIBBONS J. *Nonparametric Statistical Inference.* New York: McGraw-Hill, 1971.

GOMI H and KAWATO M. Equilibrium-point control hypothesis examined by measured arm stiffness during multijoint movement. *Science, 272:* 117-120, 1996.

GOMI H and KAWATO M. Human arm stiffness and equilibrium-point trajectory during multi-joint movement. *Biological Cybernetics, 76:* 163-171, 1997.

HAGGARD P. Perturbation studies of coordinated prehension. In Bennett K and Castiello U (Eds), *Insights into the Reach to Grasp Movement.* Holland: Elsevier Science, 1994.

HAJIAN A and HOWE R. Identification of the mechanical impedance at the human finger tip. *Journal of Biomechanical Engineering, 119:* 109-114, 1997.

HOGAN N. Impedance control: An approach to manipulation: Part I – theory, part II – implementation, part III – applications. *Journal of Dynamic Systems*, *Measurement, and Control, 107:* 1-24, 1985.

IBERALL T. Human prehension and dexterous robot hands. *International Journal of Robotics Research, 16:* 285-299, 1997.

JAKOBSON L and GOODALE M. Factors affecting higher-order movement planning: A kinematic analysis of human prehension. *Experimental Brain Research, 86:* 199-208, 1991.

JEANNEROD M. Intersegmental coordination during reaching at natural visual objects. In Long J and Baddeley A (Eds), *Attention and Performance IX.* Hillsdale: Lawrence Erlbaum Associates, 1981.

JEANNEROD M, ARBIB M, RIZZOLATTI G and SAKATA H. Grasping objects: The cortical mechanisms of visuomotor transformation. *Trends in Neurosciences, 18:* 314-320, 1995.

JOHNSON-FREY S. The neural bases of complex tool use in humans. *Trends in Cognitive Sciences, 8:* 71-78, 2004.

KAMPER D, CRUZ E and SIEGEL M. Stereotypical fingertip trajectories during grasp. *Journal of Neurophysiology, 90:* 3702-3710, 2003.

KAO I, CUTKOSKY M and JOHANNSON R. Robotic stiffness control and calibration as applied to human grasping tasks. *IEEE Transactions on Robotics and Automation, 13:* 557-566, 1997.

KIM B-H, YI B-J, OH S-R and SUH I. Non-dimensionalized performance indices based optimal grasping for multi-fingered hands. *Mechatronics, 14:* 255-280, 2004.

LEIJNSE J. Measuring force transfers in the deep flexors of the musician's hand: Theoretical analysis, clinical examples. *Journal of Biomechanics, 30:* 873-882, 1997.

LI Z and SASTRY S. Task-oriented optimal grasping by multifingered robot hands. *IEEE Transactions on Robotics and Automation, 4:* 32-44, 1988.

LI Z, ZATSIORSKY V, LATASH M and BOSE N. Anatomically and experimentally based neural networks modeling force coordination in static multi-finger tasks. *Neurocomputing, 47:* 259-272, 2002.

LIN Q, BURDICK J and RIMON E. A stiffness-based quality measure for compliant grasps and fixtures. *IEEE Transactions on Robotics and Automation, 16:* 675-688, 2000.

MARAVITA A and IRIKI A. Tools for the body (schema). *Trends in Cognitive Sciences, 8:* 79-86, 2004.

MARTENIUK R, MACKENZIE C, JEANNEROD M, ATHENES S and DUGAS C. Constraints on human arm movement trajectories. *Canadian Journal of Psychology, 41:* 365-378, 1987.

MASON C, GOMEZ J and EBNER T. Hand synergies during reach-to-grasp. *Journal of Neurophysiology, 86:* 2896-2910, 2001.

MASON M. Compliance and force control for computer controlled manipulators. *IEEE Transactions on Systems, Man, and Cybernetics, 11:* 418-432, 1981.

MEULENBROEK R, ROSENBAUM D, JANSEN C, VAUGHAN J and VOGT S. Multijoint grasping movements: Simulated and observed effects of object location, object size, and initial aperture. *Experimental Brain Research, 138:* 219-234, 2001.

MILNER T and FRANKLIN D. Characterization of multijoint finger stiffness: Dependence on finger posture and force direction. *IEEE Transactions on Biomedical Engineering, 45:* 1363-1375, 1998.

MISHRA B, SCHWARTZ J and SHARIR M. On the existence and synthesis of multifinger positive grips. *Algorithmica, 2:* 541-558, 1987.

MURRAY R, LI Z and SASTRY S. *A Mathematical Introduction to Robotic Manipulation.* Boca Raton: CRC Press, 1994.

MUSSA-IVALDI F, HOGAN N and BIZZI E. Neural, mechanical, and geometric factors subserving arm posture in humans. *Journal of Neuroscience, 5:* 2732-2743, 1985.

RAOS V, UMILTÀ MA, GALLESE V and FOGASSI L. Functional properties of grasping-related neurons in the dorsal premotor area F2 of the macaque monkey. *Journal of Neurophysiology, 92:* 1990-2002, 2004.

RILEY M AND ATKESON C. Robot catching: Towards engaging human-humanoid interaction. *Autonomous Robots, 12:* 119-128, 2002.

RIZZOLATTI G and ARBIB M. Language within our grasp. *Trends in Neurosciences, 21:* 188-194, 1998.

RIZZOLATTI G, CAMARDA R, FOGASSI L, GENTILUCCI M, LUPPINO G and MATELLI M. Functional organization of inferior area 6 in the macaque monkey. II. Area F5 and the control of distal movements. *Experimental Brain Research, 71:* 491-507, 1988.

ROSENBAUM D, LOUKOPOULOS L, MEULENBROEK R, VAUGHAN J and ENGELBRECHT S. Planning reaches by evaluating stored postures. *Psychological Review, 102:* 28-67, 1995.

ROSENBAUM D, MEULENBROEK R, VAUGHAN J and JANSEN C. Posture-based motion planning: Applications to grasping. *Psychological Review, 108:* 709-734, 2001.

SANTELLO M, FLANDERS M and SOECHTING J. Postural hand synergies for tool use. *Journal of Neuroscience, 18:* 10105-10115, 1998.

SANTELLO M, FLANDERS M and SOECHTING J. Patterns of hand motion during grasping and the influence of sensory guidance. *Journal of Neuroscience, 22:* 1426-1435, 2002.

SHIMOGA K. Robot grasp synthesis algorithms: A survey. *International Journal of Robotics Research, 15:* 230-266, 1996.

SMEETS J and BRENNER E. A new view on grasping. *Motor Control, 3:* 237-271, 1999.

SMEETS J and BRENNER E. Does a complex model help to understand grasping? *Experimental Brain Research, 144:* 132-135, 2002.

SOECHTING J and FLANDERS M. Parallel, interdependent channels for location and orientation in sensorimotor transformations for reaching and grasping. *Journal of Neurophysiology, 70:* 1137-1150, 1993.

SPEETER T. Primitive based control of the Utah/MIT dextrous hand. *IEEE International Conference on Robotics and Automation*, Sacramento, CA, 1991.

TSUJI T, MORASSO P, GOTO K and ITO K. Human hand impedance characteristics during maintained posture. *Biological Cybernetics, 72:* 475-485, 1995.

TURNER M. *Programming Dextrous Manipulation by Demonstration.* Unpublished doctoral dissertation, Stanford University, 2001.

VAN DOREN C. Grasp stiffness as a function of grasp force and finger span. *Motor Control, 2:* 352-378, 1998.

VOGEL S. *Prime Mover: A Natural History of Muscle.* New York: W.W. Norton and Company, 2001.

WASHBURN S. Tools and human evolution. *Scientific American, 203:* 63-75, 1960.

YOSHIKAWA T. Manipulability of robotic mechanisms. *International Journal of Robotics Research, 4:* 3-9, 1985.

ZACKSENHOUSE M and MARCOVICI P. Interactive recognition of simultaneous manipulative hand movements. *Mechatronics, 11:* 389-407, 2001.

ZATSIORSKY V, LI Z and LATASH M. Coordinated force production in multi-finger tasks: Finger interaction and neural network modeling. *Biological Cybernetics, 79:* 139-150, 1998.

Jason Friedman, Department of Computer Science and Applied Mathematics, Weizmann Institute of Science, POB 26, Rehovot 76100, Israel.
e-mail: jason.friedman@weizmann.ac.il